RSC Advances

This is an *Accepted Manuscript*, which has been through the Royal Society of Chemistry peer review process and has been accepted for publication.

Accepted Manuscripts are published online shortly after acceptance, before technical editing, formatting and proof reading. Using this free service, authors can make their results available to the community, in citable form, before we publish the edited article. This *Accepted Manuscript* will be replaced by the edited, formatted and paginated article as soon as this is available.

You can find more information about *Accepted Manuscripts* in the **Information for Authors**.

1   **A Metabolomics–based Approach for Ranking the Depressive Level in Chronic**

2   **Unpredictable Mild Stress Rat Model**

3

4   Xinyu Yu[a,1], Shanlei Qiao[a,b,1], Di Wang[a], Jiayong Dai[a], Jun Wang[b], Rutan Zhang[a], Li Wang[a],

5   Lei Li[a] ✉

6

7   *[a]Department of Hygiene Analysis and Detection, School of Public Health, Nanjing Medical*

8   *University, Nanjing, Jiangsu 211166, P. R. China*

9   *[b]The Key Laboratory of Modern Toxicology, Ministry of Education, School of Public Health,*

10   *Nanjing Medical University, Nanjing 211166, Jiangsu, P.R. China.*

11

12   *1 Authors contributed equally.*

13   *✉Corresponding authors:*

14   *Lei Li, Department of hygiene analysis and detection, School of Public Health, Nanjing*

15   *Medical University, 101 Longmian Avenue, Nanjing 211166, P. R. China*

16   *Tel: +86-25-8686-8404; Fax: +86-25-8686-8499; E-mail: drleili@hotmail.com*

17

18

19

20

21

22

23

24

25

26

27

28

29

30

31

32

33   **Abstract**

34   An untargeted metabolomics study to investigate the metabolome change in plasma, hippocampus and prefrontal

35   cortex (PFC) in animal model of major depressive disorder (MDD) had been conducted. Metabolomic profiling for

36   the different bio-samples was analyzed by using Ultra-High Performance Liquid Chromatography coupled with

37   Orbitrap mass spectrometry (UPLC-Orbitrap-MS). Behavioral tests were applied to evaluate the depressive degree

38   and antidepressive effect. Then the univariate and multivariate statistics including Student's t-test, principal

39   component analysis (PCA) and partial least squares discriminant analysis (PLS-DA) were applied to reveal the

40   metabolic differences between control, model and antidepressive-treated group. Metabolomics analysis

41   demonstrated that MDD was a kind of systemic disease in which disturbance of neuroendocrinology, amino acid

42   metabolism, energy metabolism, lipid metabolism and synthesis of neurotransmitter were involved. The

43   significantly changed metabolites acquired from the statistical method were identified and a simplified panel

44   which consisted of 6 metabolites including L-tryptophan, L-kynurenine, quinolinic acid, L-phenylalanine,

45   gamma-aminobutyric acid and N-Acetylaspartic acid was obtained. In combination with the results of sucrose

46   preference test, a new PLS-DA model conducted by the identified changed metabolome showed a good predictive

47   power which meant the metabolome was able to rank the depressive level as the behavioral test. Then correlational

48   analysis indicated the simplified panel in plasma had a relative good correlation with that in hippocampus and PFC.

49   This study offers a new strategy for characterization of endogenous metabolic perturbations by a metabolomics

50   method and the good predictive power and correlation for the significantly changed metabolome between plasma

51   and brain regions might be helpful in ranking the depressive level in CUMS model. These results are helpful in

52   further study to develop a noninvasive and exact diagnostic approach by an objective laboratory-based test through

53   the metabolomics platform.

54   **Key words:** metabolomics; Chronic unpredictable mild stress; UPLC-Orbitrap-MS; Biomarkers

55

56

57

58

59

60

61

62

63   **1.   Introduction**

64   Major depressive disorder (MDD) is a complex psychiatric illness which is often related to various stressful

65   events in our daily life and it has been regarded as one of the most common mental diseases around the world for

66   the prevalence of 15%-20%[1]. It has greatly influenced the life quality of more than 350 million depressive patients

67   and it is known as one of the vital cause of disability worldwide[2]. Different kinds of stressful events is experienced

68   in all human subjects during their lifetimes which can affect multiple biochemical systems and finally leads to

69   several diseases[3-5]. Moreover, it has been reported that the stressors, especially for those chronic, low intensity

70   stressful events are the most likely catalyst in the etiology of MDD[6]. For simulation of diverse chronic stressful

71   events exposure, chronic unpredictable mild stress (CUMS) model has been established and in this model, animals

72   are sequentially exposed to a series of chronic mild stressors for several weeks which aims to mimic the stress of

73   human society[7]. Therefore, CUMS model has been regarded as one of the most valid and reliable animal models

74   and has been wildly applied for the further research of MDD.

75   Metabolomics, which focuses on qualitative analysis of metabolites in biological samples at the global level,

76   has emerged as a powerful tool in the investigation of significant biochemical alterations. It has been applied for

77   capturing disease-specific metabolomic signatures and then searching for potential biomarkers in combination with

78   multivariate statistical methods which can provide new insight into deeper understanding of the pathological

79   mechanisms for diseases[5, 8]. In previous research, our group has successfully established a urine-based metabolic

80   profiling approach in CUMS rats by UPLC-MS[9], however, current researches are mostly focused on a single

81   sample such as urine, plasma or the brain tissue which can't reflect the dynamic and systemic metabolic changes in

82   the pathological process of MDD.

83   Researches have shown that the hippocampal function is closely related to short-term memory and learning

84   capacity, and the nerve cells in hippocampus are extremely sensitive to stress. Besides, it has been reported that

85   stress can also do great harm or even cause neuronal apoptosis in certain brain regions, especially for hippocampus.

86   Moreover, the Magnetic Resonance Imaging (MRI) of the depressive patients also demonstrated a reduction in the

87   volume of hippocampus[10-12]. So there is increasing evidence indicated that hippocampus plays an important role in

88   the pathogenesis of depression.

89   The prefrontal cortex (PFC) is one of the last brain regions to mature fully during ontogenesis which plays a

90   key role in regulation function in central nervous system. The function of PFC is mainly associated with long-term

91   memory, expression of emotions and spatial cognition and it was very sensitive to various damage[13]. The

92   dysfunction of PFC have been proved to have a close relationship with many psychiatric disorders including

93   post-traumatic stress disorder, bipolar disorder and MDD. The working memory which could be defined as the

94   gradual development of memory system from short-term to long-term memory and it was more closely correlated

95   to PFC than hippocampus and basal ganglia[14]. Electrophysiological and neuroimaging studies had been applied to

96   explore the function of PFC in the formation of long-term memory and pathogenesis for diseases and indicated that

97   due to the character of pyramidal neuron in PFC, it could keep the message even when stimulus disappeared[15, 16]. It

98   had been reported that there was a decreased cerebral blood flow along with the energy metabolic disturbance in

99   MDD patients, and neuroimaging indicated a reduction in volume for PFC grey matter[16]. Besides, dysfunction of

100   neurotransmitters and metabolic changes for amino acid was observed by metabolomic methods in CUMS

101   animals[17].

102   However, the essential prerequisites for the biomarkers which can be applied in the diagnosis of diseases are

103   that they are of relatively high sensitivity and accuracy, and the testing sample should be easily obtained. For

104   MDD, brain biopsy samples are neither practical nor convenient, while for plasma samples, it can be easily

105   collected at minimal risk and cost to the patient. So it is necessary to explore whether the metabolic changes in

106   plasma are consistent with those in brain, especially in hippocampus and PFC.

107   In this study, we collected three kinds of samples, plasma, hippocampus and PFC from control, CUMS model

108   and antidepressant-treated rats in order to investigate the pathogenesis of MDD according to the metabolome

109   change from peripheral blood to CNS by a UPLC-Orbitrap-MS based metabolomics platform. Then we also aimed

110   to establish an objective method to rate the level of depression by matching results of behavioral test and the

111   changed-metabolome. Finally, according to the mutual changed metabolites in three kinds of samples, we

112   simplified the biomarkers to a panel, and then explored whether changed level of metabolites in the simplified

113   panel was associated with results of behavioral test. In order to investigate whether it was practical to use the

114   simplified panel in plasma to represent that in brain, correlation analysis was also performed to explore the

115   relationship between the panels in three kinds of samples.

116

117   **2.   Materials and Methods**

118   **2.1 Chemicals and Reagents**

119   HPLC grade methanol, acetonitrile and formic acid were purchased from Merck (Merck, Darmstadt,

120   Germany). Deionized water was produced by Milli-Q50SP Reagent system (Millipore Corporation, MA, USA).

121   Paroxetine hydrochloride was obtained from Sigma-Aldrich (MO, USA). The enzyme linked immunosorbent

122   assay (ELISA) kits of rat IL-6 and TNF-α were obtained from 4A biotech Co.Ltd. (Beijing, China).

123   **2.2 Animals**

124   30 male Wistar rats, weighing $100 \pm 10g$ were commercially purchased from Shanghai Laboratory Animal Co.

125   Ltd. (SLAC, Shanghai, China). All rats were housed individually and kept at a laboratory animal barrier system

126   with required environment (temperature of $24\pm1°C$, relative humidity of $45\pm15\%$, and a 12h light/dark cycle). Rats

127   were allowed to acclimatize the environment for two weeks and during this period, every rat had free access to

128   standard rat chow and tap water. The study was approved by national legislations of China and local guidelines and

129   the experiments were performed according to a protocol approved by the Nanjing Medical University Institutional

130   Animal Care and Use Committee.

131   **2.3 Chronic unpredictable mild stress (CUMS) protocol**

132   After two weeks of acclimatization, the rats were firstly trained to consume the 1% sucrose solution, and this

133   training lasted for three weeks. During the training period, the sucrose preference test (SPT) was conducted twice a

134   week in the first 2 weeks and once in the last week until the sucrose preference (SP) of each rat was stable. Then

135   the rats were randomly divided into three groups, control group, model group and model group treated with

136   paroxetine, and each group contained 10 rats. During the whole experience, rats in control group were fed with

137   food and tap water *ad libitum*, except for a 20h food and water deprivation before each SPT. According to the

138   experimental design shown in Fig,1, in the first three weeks, rats in model and treated group were exposed to a

139   series of chronic unpredictable mild stressors according to the protocol which has been changed slightly. The

140   stressors consisted of 45°cage tilting along the vertical axis, paired housing, food or/and water deprivation,

141   stroboscopic illumination (200 flashes/min), soiled cage (300 ml water spilled into the padding), continuous

142   overnight illumination, and white noise (85db). The detailed schedule was displayed in S-Table.1. Then, rats in

143   treated group received antidepressive drug administration, and rats in both model and treated group were still

144   exposed to the CUMS procedure in the next 4 weeks. The paroxetine was dissolved in physiological saline and

145   administrated intraperitoneally at the dosage of 10mg/kg at 9:00 every morning. Rats in another two groups

146   received administration of physiological saline in the same volume.

147   **2.4 Behavioral test**

148   2.4.1 Sucrose preference test

149   According to Willner who firstly conducted the CUMS model, the Sucrose preference test (SPT) was selected

150   as an intuitively measurement of anhedonia in rats which exposed to a series of stressors[18, 19] . Before each test, all

151   rats were deprived of water and food for 20h, then they were put into individual cages and provided with two

152   bottles of different solution, tap water and 1% sucrose solution. During this 2-hour-long test, rats were staying in

153 normal environmental without any stressors mentioned above and they had free access to two kinds of solution.

154 Bottles with tap water and sucrose solution were switched once an hour to avoid the place preference.

155 The SP means the ratio of consumed 1% sucrose solution relative to that of total solution in the test, and can

156 be calculated according the formula below:

157 SP = sucrose consumption/ (sucrose consumption + water consumption) *100%

158 2.4.2 Open-field test

159 The open-field test (OPT) was conducted to evaluate the ability of spatial exploration[20]. All rats were

160 transferred to a quiet operating room (<65d) 30min before each test for acclimatization and then the test was

161 conducted between 13:00 and 16:00. Each rat was gently put into the test field which consisted of black

162 background marked with a grid dividing it into 25 equal-size squares ($100*100\ cm^2$) and a 40-cm-high wall. After

163 adaption for 30s, then the rats took the 5-minutes-long test, and a record was kept of the locomotor activity such as

164 the time spent in the center square and the frequency of rearing (standing upright on one's hind paws).After each

165 rat' test, the open field was clean by 75% ethanol to eliminate the smell and faeces.

166 2.4.3 Forced swimming test

167 The forced-swimming test (FST) was performed as a valid measurement when evaluating the status of

168 depression for animals undergoing CUMS procedure[21]. Rats were individually put into Plexiglas cylinders (50cm

169 in height and 18cm in diameter) which filled with water ($25\pm1\ ^{o}C$) up to a height of 20cm. The cylinder was

170 thoroughly cleaned after each test. During the 5-minutes-long test, the total immobility time was recorded with the

171 help of chronograph.

172 2.4.4 Food consumption and body weight.

173 During the whole experiment, the consumption of chow for each rat was recorded, and specifically, at 17:00

174 every afternoon, fresh chow was weighed and added into the feeding trough, then after 24h, we removed the

175 uneaten chow and weighed it. Food consumption was recorded everyday as a measurement of appetite and body

176 weight of each rat was recorded once a week.

177 **2.5 Statistical Analysis for behavioral data**

178 All data from behavioral test was expressed in the form of mean±standard deviation. The statistical analysis

179 was carried out by using SPSS 17.0 software (Chicago, IL, USA). The results of OPT was non-normal-distributed

180 so the Kruskal-Wallis test was applied to analyze it, while for the results of other behavioral tests including SPT,

181 FST, food consumption and body weight, they were analyzed by one-way analysis of variance (ANOVA) followed

182 by post hoc LSD test. The significance level was set at $p<0.05$.

183   **2.6 Sample collection and preparation**

184   According to the experimental schedule, as soon as the final behavioral test finished, the blood samples were

185   obtained from portal vein and collected in heparin sodium anticoagulation tubes. Then rats were sacrificed and the

186   hippocampus and PFC were dissected from brain on ice, weighed, frozen with liquid nitrogen rapidly. The blood

187   samples were firstly centrifuged at 3000 rpm for 10 minutes and then collected the supernatant. All the samples

188   were stored at -80°C immediately.

189   Prior to analysis, all samples were thawed at room temperature for the following preparation. 500μl plasma

190   samples were mixed with acetonitrile at the ratio of 1:3 (v/v) and centrifuged at 12,000 rpm for 20 minutes to

191   remove large-molecular-weight proteins. Then the supernatants were diluted with water at a ratio of 1:3 (v/v) again

192   and transferred to vials for metabolomic profiling.

193   For hippocampus and PFC samples, 20mg of each sample was transferred to a 2ml centrifuge tube and mixed

194   with 1ml extracting solution of water-acetonitrile-chloroform (2:5:2, v/v/v). The mixture was then blended by

195   Tissue Lyser II (Dusseldorf, Germany) at the frequency of 50Hz for 15 minutes, subsequently centrifuged at

196   12,000 rpm for 10 min and 600μl supernatant was transferred to vial for analysis.

197   **2.7 UPLC-Orbitrap-MS analysis**

198   The chromatographic separation was performed on a UPLC Ultimate 3000 system (Dionex, Germering,

199   Germany) equipped with a 1.9μm Hypersile Gold C_{18} column (100mm×2.1mm) (Thermo Fisher Scientific), and

200   the column was maintained at 40°C. A multistep gradient consisted of 0.1% formic acid in water (A) and 0.1%

201   formic acid in acetonitrile (B) had been applied and the gradient operated at a flow rate of 0.4 mL/min by linearly

202   increasing solvent B from 5% to 95% over 15 min, then the column was washed with 95% solvent B for 2 min and

203   re-equilibrated in 5% solvent B. The UPLC autosampler temperature [Ultimate WPS-3000 UPLC system (Dionex,

204   Germering, Germany)] was set at 4°C and the injection volume for each sample was 5 μL.

205   MS data were collected by the Orbitrap mass spectrometer (Thermo Fisher Scientific, Bremen, Germany)

206   equipped with a heated electrospray source (HESI) at the resolution of 700,000 in both positive and negative mode

207   simultaneously. For both positive and negative mode, the operating parameters were set as follows: a spray voltage

208   of 3 kV, the capillary temperature of 300°C, sheath gas flow of 40 arbitrary units, auxiliary gas flow of 10 arbitrary

209   units, sweep gas of 2 arbitrary units and S-Lens RF level of 50. In the full scan analysis (70 to 1050 amu), the

210   resolution was set at 700,000 with an automatic gain control (AGC) target of $1×10^6$ charges and a maximum

211   injection time (IT) of 120 ms. Both the UPLC and the Orbitrap mass spectrometer system were controlled by the

212   Xcalibur 2.2 software (Thermo Fisher Scientific).

213   The quality control (QC) samples had been prepared by pooling same volume of supernatant from samples of

214   plasma, hippocampus and PFC, respectively and were pretreated in the same manner as real samples, then

215   analyzed every 10 samples to ensure the stability and repeatability. The mass spectrometry was calibrated every 24

216   hour during the profiling to ensure the mass accuracy.

217   **2.8 Data analysis**

218   All of the raw data files were introduced to the SIEVE software (Thermo Fisher Scientific) where data

219   pretreatment including peak realignment, baseline correction and peak deconvolution had been done. After data

220   pretreatment, a table which was organized into a three-dimensional matrix consisted of sample names

221   (observations), annotated peak indices (RT-m/z pairs) and the intensity of each sample (i.e. peak area) had been

222   obtained. The data was then mean-scaled and imported into the SIMCA-P 13.0 software (Umetrics, Umea, Sweden)

223   for multivariate statistics such as principal component analysis (PCA) and partial least squares discriminant

224   analysis (PLS-DA). PCA reduced high dimensional spectral variation into a two or three principal components

225   without losing the vast majority of information, and then the score map visualized the distribution of the clustering

226   or the grouping in the observations. PLS-DA was then performed to improve the classification, offer pairwise

227   comparison and search for the variable importance in the projection (VIP) to identify the significantly changed

228   variables induced by CUMS procedure. Dataset acquired from control and model group was applied to conduct a

229   new PLS-DA model as the training set, and that of treated group was then used to validate and test the predictive

230   ability of the model in conjunction with the results of behavioral tests. Variables with VIP values larger than 1.0

231   were considered as statistically significant in this model and they were supposed to be the metabolites which

232   counted most in the discrimination between groups. Furthermore, unpaired Student's t-test was carried out for the

233   normalized data and in general, the variables with VIP value larger than 1.0 and q-value less than 0.05 were

234   deemed to be statistically significant. Those variables were then identified according to their m/z and retention

235   time in the following analysis.

236   In order to explore whether the level of metabolites could reflect the severity of anhedonia in CUMS model, then

237   we studied the association between the changed metabolome and the result of behavioral test. Compared with OPT

238   and FST, the result of SPT varied within a small range, suggesting it was more stable and accurate and it was

239   widely used in CUMS model as a measurement of depressive state, so we defined SP as the Y variable and the

240   metabolic dataset of training set (control and model group) was set as the X variable in the new PLS-DA model

241   and then the dataset of treated group was put into the model as a test set to further validate the performance of the

242   model. The predictive ability and whether the changed metabolome in the simplified panel could reflect the

243   depressive level had been tested, and a permutation test for that model was conducted to confirm it.

3.   Results

3.1 Behavioral test

246   Following the CUMS procedure, the SP of each rat was shown in Fig.2a. Significantly decreased SP had been

247   observed after three weeks' CUMS procedure. While in the following 4 weeks, the SP of model group turned out a

248   sustained downward trend compared with control group, and for that of treated group, it began to rise gradually

249   and at the final SPT, it achieved statistical significance compared with model group. The OPT had been done twice

250   according to the schedule and the results were displayed in Fig.2b,c. The locomotor activities including rearing

251   frequency and the time spent in the central square were recorded to reflect the status of depression. The rearing

252   frequency of rats in model and treated group was significantly decreased compared with control group, while rats

253   received antidepressant treatment, situation was getting better compared with rats without treatment at week 7 and

254   the results of time spent in the central square turned out similar tendency. Previous researches showed that

255   significant reduction of rearing frequency could indicate decreased exploratory behavior, and the time spent in

256   central sector could reflect the degree of anxiety in rodent[22, 23]. The immobility time in the FST (Fig.2d.) was

257   obviously increased in model and treated groups compared with control group after CUMS exposure. Moreover

258   there was no statistical difference significant difference ($p>0.05$) between control and treated group at week 7, and

259   it may indicate that the immobility time in FST was closely related to desperation and could reflect the depressive

260   state to some extent. Therefore, according to the results of behavioral tests, the significant decrease for SP, affected

261   locomotor activities and the longer immobility time in FST demonstrated that depressive–like behaviors

262   impairment of hedonic reactivity and anhedonia did occur which meant the model had been successfully

263   conducted.

264   CUMS procedure also resulted in a reduction of food consumption and further led to the significant decrease

265   of body weight in model rats compared with control rats, and this situation improved after antidepressive treatment.

266   The body weight of three groups was displayed in supplementary information (S-Fig.1), and the detailed data was

267   presented in S-Table.2.

3.2 Metabolomics profiling

269   Metabolic profiling was conducted according to the chromatographic and mass spectrum conditions described

270   above. To explore the differences between groups, multivariate analysis was performed which help to reduce the

271   data to a low dimensional space where discrimination of metabolomic profiles between sample classes can be

272   modeled. To ensure the stability and repeatability of equipment, the PCA score plots of QC samples were firstly

273   analyzed to evaluate the general situation of analyzing process. The PCA score plots (S-Fig,2.) indicated that the

274   equipment was stabile during the processing and the reliable data was then used for subsequent multivariate

275   analysis. A total of 4926 (3754 in positive mode and 1172 in negative mode), 4342 (3440 in positive mode and 902

276   in negative mode) and 3813 (2990 in positive mode and 823 in negative mode) features were obtained in the

277   samples of plasma, hippocampus and PFC, respectively. For pre-treated dataset of plasma, a PCA model was

278   achieved which accounted for 47.7% of the total variations in the first three components. Besides, for hippocampus

279   and PFC, 41.2% and 37.8% of the total variations were accumulated within the first three components, respectively.

280   According to the score plots displayed in Fig.3, relative clear separation between control and model group could be

281   obtained which preliminarily indicated metabolic pattern did changed in those samples.

282   To improve classification, a more sophisticated multivariate model, PLS-DA was performed to maximize

283   discrimination between the three groups. The score plots of PLS-DA model showed a clearly discrimination

284   between groups and the key parameters were displayed in Table.1. Briefly, both R^2Y and Q^2 which were employed

285   to quantify the goodness-of-fit and predictability were greater than 0.5, suggesting that this model was predictive

286   and robust[24, 25]. According to the score plot, the cluster of treated group was apparently moving towards to that of

287   control group in the first component which was consistent with the results of behavioral tests, suggesting the

288   severity of depression had been improved.

289   **3.3 Searching for discriminate variables**

290   The variable importance for projection (VIP) value which signified the influence of variables on the

291   classification was obtained from PLS-DA model. Then the VIP value, along with p-value acquired from the

292   Student's t test was applied for the selection of discriminational variables between three groups. The variables with

293   VIP values larger than 1.0 and p-value less than 0.05 was chosen as the candidate biomarkers and then be

294   identified[24].

295   **3.4 Metabolite identification**

296   The selected variables which were significantly changed after the CUMS exposure according to VIP-value

297   and p-value were presented in the form of m/z and retention time pairs. Our library had established an in-house

298   library which consisted of 493 authentic chemicals and analyzed in the pre-described conditions with high accurate

299   m/z and retention time. While for those variables without authentic chemicals, the online commercial database

300   including Human Metabolome Database (HMDB version 3.6) and KEGG was searched to putatively identify in

301   the tolerance of 3 ppm according to metabolite identification confidence defined by the Metabolomics Standards

302   Initiative[26]. The metabolites for both confidently and putatively identified in plasma, hippocampus and PFC

303   samples were listed in Table.2,3,4, respectively, and the retention time shift of each metabolites with authentic

304   chemicals was displayed in S-Table.3,4,5, respectively.

305   However, it was inconvenient and unpractical for diagnosis based on quantification of so many metabolites,

306   so we attempted to search for a simplified metabolite panel in order to represent for the discriminatory power of

307   most metabolites. Moreover, our primary goal is to explore whether there was a temporal relation of metabolome

308   changing from plasma to brain such as hippocampus and PFC, so in this study, we chose the mutual metabolites in

309   plasma, hippocampus and PFC samples. Then in order to explore whether the simplified panel in plasma could

310   correctly reflect the metabolome change in brain, correlation analyses of metabolites in the simplified panel

311   (plasma versus hippocampus and plasma versus PFC) were performed and the plots were displayed in S-Fig.3. The

312   plasma metabolite intensities were correlated with hippocampus metabolite intensities and PFC metabolite

313   intensities, respectively. The scatter diagrams of each metabolites in that panel were displayed in Fig.4, and the

314   calculated Pearson's coefficient values and p-values were shown in Table.5, which indicated a better correlation for

315   panel in plasma with that in hippocampus. Furthermore, we also investigate the correlation between SP and

316   metabolite intensities in the simplified panel to explore the associations of metabolites in simplified panel with

317   disease severity indices and whether the panel could relate the overall metabolome change with the result of

318   behavioral test. The metabolite intensities were mean-scaled to reduce the impact for the difference in the order of

319   magnitude and the results demonstrated that the panel in plasma could basically satisfy the requirement (Fig.5) and

320   the coefficient values and p-values were displayed in Table.6. Specifically, L-kynurenine, quinolinic acid,

321   L-phenylalanine and N-acetyl-L-aspartic acid were negatively associated with the SP (r=-0.70, -0.73, -0.79, -0.74,

322   respectively), indicating that higher level of these compounds in plasma was associated with severer level of

323   melancholic symptoms. Besides, the level of L-tryptophan, gamma-aminobutyric acid and was positively

324   associated with SP which suggested that model rats with more symptoms of anhedonia had lower level of those

325   metabolites in plasma.

326   In general, according to the Pearson's correlation coefficients, we may draw the conclusion that, the changing

327   tendency of simplified panel in plasma was almost the same as that in hippocampus and PFC which indicated the

328   simplified panel in plasma could partly reflect the changed metabolome in brain. Moreover, we also found the

329   correlation between the normalized dataset of the panel in plasma and SP was relatively good.

330   The result that whether the simplified could rank the depressive level was displayed in Fig.6. The score plot

331   of the new model conducted by the dataset of training group was shown in Fig.6a which also demonstrated a very

332   clear separation between control and model group. In the predict plot of the new fitted model (Fig.6b), the Y axis

333   was the SP acquired from behavioral test, and the X axis was a predicted SP calculated by the model. According to

334   the predict plot, when the test set was put into the new PLS-DA mode, the predicted SP was almost was close to

335   the real SP, indicating that the PLS-DA model was robust and had a relative good predictive power when facing

336   new observations. Furthermore, to rule out nonrandomness of separation, a 50-iteration permutation test (Fig.6c)

337   was performed and the corresponding values from the permutation test were lower than the original value which

338   further validated the model.

339   **4.   Discussion**

340   Nowadays the diagnosis of MDD is mainly rely on symptom-based assessment such as Hamilton depression

341   rating scale (HAMD), in other words the lack of biomarkers which can lucubrate the pathogenesis and further

342   support laboratory-based diagnosis remains a bottleneck in the study and prevention of MDD. In this study, we

343   further explored the metabolome changes in multiple samples in order to find a simplified metabolites panel in

344   plasma which can reflect the metabolome changes in hippocampus and PFC more directly and accurately than our

345   previous urinary metabolomics study. Moreover, we also studied the association between the changed metabolome

346   and the result of behavioral test for the purpose of exploring whether the level of metabolites could reflect the

347   severity of anhedonia in CUMS model. Generally, these results demonstrated that the changed metabolome was

348   able to rate the depressive level in CUMS rats and it was promising and practical to evaluate the severity of MDD

349   by a more objective laboratory-based metabolomics method in conjunction with behavioral tests. Finally, in this

350   study, a UPLC-Orbitrap-MS based metabolomics profiling was conducted to capture the significantly changed

351   metabolites in plasma and brain samples, then the understanding of these metabolites could provide new insights

352   into underlying the pathogenesis and promote the discovery of biomarkers which could be used in the diagnosis or

353   precaution for MDD.

354   4.1 CUMS-induced metabolomic changes

355   After the exposure of CUMS procedure, metabolic changes were observed and the changed metabolome was

356   mainly involved in the amino acids metabolism, lipid metabolism, energy metabolism, oxidative stress and

357   endocrine metabolism shown in Fig.7. According to the mutual metabolites in plasma, hippocampus and PFC, we

358   simplified the changed metabolome into a panel consisting six metabolites. Considering the practicability of the

359   biomarkers in the future research of diagnosis, we placed more emphasis on the biointerpretation of metabolites in

360   the simplified panel along with corticosterone which could connect the changed metabolome between plasma and

361   brain. Moreover, we also gave detailed biochemical interpretation for the remaining significantly-changed

362   metabolites in supplementary information.

363   The significantly changed level of tryptophan (Trp) and its metabolites kynurenine (Kyn), kynurenic acid

364   (KYNA), quinolinic acid (QUIN) and 5-hydroxyindoleacetic acid (5HIAA) was observed after CUMS procedure

365   in model group. Trp was an essential amino acid in our body which acted as the precursor of serotonin. The

366   serotonin was a local transmitter at synapses which acted as the biochemical messenger and regulator in the central

367   nervous system and it had been proved that the significantly decreased level of serotonin had a close relationship

368   with MDD according to the monoamine neurotransmitter hypothesis. In addition to participating in the

369   biosynthesis of proteins, Trp could be catabolized in two main pathways: Kyn pathway and serotonin (5-HT)

370   pathway. For the Kyn pathway, Trp was firstly converted into N'-formylkynurenine by indoleamine-2,

371   3-dioxygenase (IDO) or L-tryptophan-2, 3-dioxygenase (TDO). It had been reported that the increasing

372   proinflammatory cytokines like IL-6 and TNF-α can active IDO[27], and then the activation of Kyn pathway would

373   result in that more Trp was then catabolized into formylkynurenine, while for serotonin pathway, the decline of Trp

374   would cause the decrease of its metabolites serotonin. Moreover, even though the serotonin hadn't been detected in

375   this study, the level of its main breakdown product 5-HIAA was significantly decreased which might partly due to

376   the down-regulation of serotonin. Interestingly, according to the results of ELISA (S-Fig.4), the levels of IL-6 and

377   TNF-α was significantly higher in the plasma of model rats and this validated the activation of Kyn pathway and

378   moreover, it also indicated MDD would be an inflammatory disease which offered the chance to have a new

379   understanding of MDD in a new perspective. Additionally, the decreased level of Trp, along with the significantly

380   increased level of Kyn and its catabolite QUIN also demonstrated the metabolism of Trp was mainly converted

381   into Kyn pathway.

382   When the metabolism of Trp was converted into Kyn pathway where the metabolites had appreciable effect

383   on the neuroprotective–neurodegenerative balance in the brain. Kyn could be furthered catabolized by two

384   pathways: the toxic quinolinic pathway where several excitotoxic metabolites were produced and the kynurenic

385   pathway. In quinolinic pathway by the function of kynurenine-3-monoxygenase, Kyn could be catabolized in to

386   3-hydroxy kynurenine (3-HKK) which proved to be an endogenous excitotoxin and the bioprecursor of QUIN. It

387   could generate free radical which was able to cause damage to the function of brain including the apoptosis of

388   neurons or some neurodegenerative changes. For QUIN, it was a kind of NMDA receptor agonist which was

389   produced by microglial cell. And it was associated with several psychiatric and neurodegenerative disorders

390   including Parkinson's disease, MDD and Alzheimer's disease[28, 29]. It had been reported that cytokines could induce

391   an increase for QUIN in the plasma and cerebrospinal fluid of MDD patients and the significantly evaluation of

392   proinflammatory cytokines in plasma had been observed in CUMS model rats which was consistent with previous

393   studies[28]. In the condition of nerve inflammation, QUIN could over-activate NMDA receptor and inhibit the

394   resorption of glutamic acid (Glu) for gliocyte which worsen the excitotoxin of Glu in central nervous system.

395   When the level of QUIN gradually increased and reached the pathological level, it could affect the function of

396   neuron or even induce apoptosis. Additionally, QUIN was also able to produce the toxic effects by lipid

397   peroxidation or undermining the stability of neuronal cytoskeleton. Under normal condition, astrocyte could

398   reabsorb the released Glu by synapse, then convert Glu to glutamine (Gln) and finally release Gln to presynaptic

399   membrane in order to regulate the level of Glu. However, the increased level of QUIN was capable to cause a

400   reduction for glutamine synthetase, leading to a turbulence of the regulation for Glu in astrocyte and leading to

401   accumulation of Glu. Glu had been widely accepted as an excitatory neurotransmitter, consisting in all neurons in

402   CNS and the dysregulation or over-activating its receptor would finally had a bad effect on neurons. As was

403   mentioned, the evaluation of QUIN along with the accumulation of Glu would over-activate the NMDA receptor,

404   producing the synergetic effect and intensifying the excitotoxic effect in CNS. Worse still, the decrease for

405   astrocyte led to an increase of proinflammatory cytokines which then further activated the Kyn pathway and

406   resulted in a vicious cycle. Studies had shown that antagonist of metabotropic glutamate receptor1 (mGluR1) and

407   NMDA could alleviate the damage of QUIN[30]. In the animal model, when received injection of AIDA or MK-801

408   could down-regulation of QUIN and relieve some depressive symptoms[31]. We could deduce that the stress-induced

409   immune response regulation resulted in an increase of proinflammatory cytokines which further led to the

410   activation of Kyn pathway and the evaluated-level of QUIN. Based on this result, we could further look into the

411   association between QUIN and Glu and have a deeper understanding of the mechanism of MDD from a new

412   perspective.

413   Kyn was also be able to be catabolized into KYNA which proved to be a well-known endogenous antagonist

414   of the NMDA receptor and maintained the balance of neuroprotective–neurodegenerative metabolites. However,

415   the pathological level of QUIN which caused the apoptosis of astrocytes as mentioned above, it could lower

416   neuroprotective activity and resulted in the decreased level of KYNA which was observed in our study. The

417   changed balance indicated a metabolic disturbance involved in MDD. In contrast to QUIN, KYNA was a

418   neuroprotective metabolite as a NMDA receptor antagonist which could mediate glutamatergic hypofunction.

419   Studies had focused on it to explore the relationship between its neuromodulatory character and the pathogenesis

420   of several CNS diseases. It had been reported that different patterns of abnormalities in KYNA metabolism was

421   observed in Huntington's disease and Alzheimer's disease[32, 33]. There was evidence that KYNA was associated with

422   cognition and memory for the impairment of cognitive function in various neurodegenerative disorders was

423 accompanied by metabolism alteration of KYNA. Our research indicated a significantly down-regulation of

424 KYNA in model group and in combination with the significantly up-regulation of QUIN, suggesting that the

425 metabolism of Kyn was mainly going into the toxic quinolinic pathway which led to an imbalance in the

426 neuroprotective and neurodegenerative metabolites in CNS.

427   Phenylalanine (Phe) was an essential amino acid which was involved in the synthesis for cellular proteins and

428 it was also the precursor for the amino acid tyrosine (Tyr) because of the similarity in structure. Phe could be

429 firstly metabolized into Tyr by hydroxylation under the function of phenylalanine hydroxylase in liver, then as a

430 precursor for L-dopa, Tyr was able to be further metabolized to several neurotransmitters like dopamine,

431 norepinephrine and epinephrine. It had been reported that MDD patients showed a significantly higher Phe-Tyr

432 than healthy control while under normal circumstances half of Phe was supposed to convert into the biosynthesis

433 of Tyr, suggesting there might be a dysfunction of related enzymes[34]. The increased level of Phe along with the

434 decreased level of Tyr observed in our research was consistent with former study. Additionally, as a precursor for

435 neurotransmitters, it shared the transport system across the blood-brain barrier with tryptophan. The metabolic

436 alteration of Tyramine, L-dopa and its metabolites dopamine and homovanillic acid (HVA) was also been observed

437 in model rats which demonstrated the turbulence in Tyr metabolism and this was supported by monoamine-based

438 mechanism for MDD. Then due to the metabolic disturbance of Phe and Tyr, in combination of the lower

439 concentration of dopamine and HVA, we speculated the biosynthesis for neurotransmitters in was influenced in the

440 pathogenetic process of MDD. Further study could be conducted by using targeted electrochemistry-based

441 platform to interrogate perturbations in the neurotransmitter pathways involving, dopamine, epinephrine and

442 norepinephrine to discover the association between monoamine neurotransmitters and MDD.

443   Gamma-aminobutyric acid (GABA) proved to be an inhibitory neurotransmitter which acted on inhibitory

444 synapses in CNS. It was involved in the regulation of neurotransmitters for amines, peptides and amino acids by

445 linking with specific receptors for pre or post synaptic neurons. This binding caused the opening of ion channels to

446 allow either the flow of negatively-charged chloride ions into the cell or positively-charged potassium ions out of

447 the cell. This will typically resulted in a negative change in the transmembrane potential, usually causing

448 hyperpolarization. Unlike monoamine neurotransmitter, GABA existed in almost 50% of synapsis and could be

449 metabolized by Glu via glutamate decarboxylase. It had been proved in animal models that GABAergic

450 innervation was able to suppress the secretion of corticotropin releasing hormone (CRH) in paraventricular

451 nucleus[35]. CRH was a key metabolite in the activation of hypothalamus-Pituitary-adrenal (HPA) axis and the

452 evaluation of CRH could lead to an over-activation of HPA axis which was vital in the pathogenic process of MDD.

453   In CUMS model, a reduction of GABAergic innervation had been observed, sequentially the inhibiting effect of

454   GABA for CRH iminunoreactive neuron, while after injection of CRH antagonist the depressive symptoms

455   improved. Previous studies showed a higher level of Glu in occipital cortex and a lower level of GABA in MDD

456   patients and the level of GABA was in inverse proportion of Glu in the same brain region[36]. Additionally, drugs

457   which was capable to increase the level of GABA or acted as the agonists of GABA receptors had been reported

458   had anti-anxiety and anti-convulsive effects. A significantly decreased level of GABA might indicate the

459   dysfunction of GABA synthesis and this was partly due to the reduction of glutamatergic stimulation and the

460   aberrant activity of glutamic acid decarboxylase which cause a block for Glu to convert into GABA. Moreover, the

461   lower activity of glutamic acid decarboxylase was observed in MDD patients and even some environmental factors

462   was also able to have an impact on glutamic acid decarboxylase.

463   N-Acetylaspartic acid (NAA) was a derivative of aspartic acid by acetylization and it was a high-activity

464   neuropeptide in brain. Its precursor aspartate was derived from TCA cycle and involved in energy production.

465   NAA was the second most concentration compound in the CNS for mammals just next to that of Glu. NAA was

466   biosynthesized in by aspartic acid and acetyl-coA in neuronal mitochondria. It could act as a neuronal osmolyte to

467   maintain the fluid balance in brain and it was also involved in the biosynthesis for lipid and myelin in

468   oligodendrocytes. Additionally, it was also a precursor for the synthesis of the important neuronal dipeptide

469   N-acetylaspartylglutamate. NAA was recognized as a marker for the integrity and viability of neuronal, under

470   normal circumstances, NAA was able to be transferred from neuron to oligodendrocyte and thus to clear the

471   redundant free NAA. Interestingly, the dysregulation of NAA in brain and plasma was not consist with each other

472   in previous studies[37, 38]. In oligodendrocyte, part of NAA was catabolized and synthesized the fatty acids and

473   steroids. However, when under pathological states, it could induce an increasing release for NAA due to the

474   damage of neuron and the evaluated level was firstly converted into astrocyte and then transferred to the

475   bloodstream. Moreover, astrocyte played an important role in the formation of the blood-brain barrier, and

476   extracellular NAA could be absorbed by astrocyte-expressed transporter. The dysfunction of the reabsorption for

477   NAA could also be responsible for the abnormal level of NAA in plasma, while the decreased levels of NAA in

478   brain might imply the deficits in neuronal activity and the function of mitochondrial. Generally, the increased level

479   of NAA in plasma along with the reduction of that in hippocampus and PFC might partly indicated a dysregulation

480   for NAA and a pathological state in model rats.

481   Corticosterone (CORT) is an adrenocortical steroid that has modest but significant activities as a

482   glucocorticoid. There was a great deal of researches had proved that when exposed to long-tern stressors, the

483 activity of neurosecretory system increased and manifested the hyperfunction for hypothalamic–pituitary–adrenal

484 (HPA) axis which led to an increasing level of glucocorticoid[39, 40]. A notable evaluation of cortisol had been

485 observed in many studies which focused on concentration of glucocorticoids in the blood of MDD patients. In our

486 study, the level of another kind of glucocorticoid, CORT was significantly increased and it was the main existing

487 form for glucocorticoid in rodents. Moreover, long-term injection of CORT had been proved as another effective

488 method to induce depressive-like action which was widely applied in the development of anti-depressive drugs.

489 Study had showed that after long-term injection of CORT, both the synaptophysin (SYP) which was a marker for

490 plasticity of neuron structure and brain-derived neurotrophic factor (BDNF) were down-regulated which further

491 induced dysfunction of neuron[41]. Additionally, cerebral glycogen was responsible for providing energy in neuronal

492 activity and the dysfunction of neuron in early stage was also partly due to metabolic disturbance of energy. SYP

493 was a kind of calcium binding membrane protein which had close relationship with structure and function for

494 synapse and research indicated that CORT could suppresses the generation of nervous system and then reduce the

495 density for hippocampal dendritic spines which resulted in a dysfunction of the spatial learning and memory. So

496 the increasing level of CORT could be involved in formation and development of synapse, while the decreased

497 synapse and diminished function had an effect on the information dissemination in CNS. Besides, glucocorticoid

498 was able to directly influence glycogen metabolism of astrocyte and CORT could cause a notable reduction of

499 glycogen in astrocyte. The decreased concentration of glycogen was associated with the metabolism and function

500 of astrocyte. The deficiency of glycogen in astrocyte might further result in neuron apoptosis which could affect

501 the metabolism of neurotransmitters and the transmission of action potential.

502 Hypothalamic–pituitary–adrenal (HPA) axis played a key role in response to various kinds of stress. When

503 stress signals reached thalamic paraventricular nucleus, it would lead to a secretion for corticotropin releasing

504 hormone (CRH)[39]. Then the release of CRH would promote the generation of adrenocorticotrophic hormone

505 (ATCH) by anterior pituitary which further promote the release of glucocorticoid in order to cope with stress.

506 Hippocampus was not only a sensitive region for stress-induced damage but also a regulation center for HPA axis.

507 Hippocampus could inhibit the stress reaction and make the over-activated HPA axis return to normal. However,

508 there were abundant receptors of glucocorticoid in hippocampus so it was very sensitive to the level of

509 glucocorticoid while the increasing CORT would cause damage to hippocampal synaptic plasticity. When

510 superfluous glucocorticoid in plasma passed through blood brain barrier and acted on the receptors in brain,

511 degenerative feedback was generated by hippocampus to inhibit the activity of HPA axis to maintain hormonal

512 balance. However, when long-term exposure to high level of glucocorticoid caused an over-activity of

513 glucocorticoid receptors which further led to a weakening effect for the degenerative feedback. Worse still, the loss

514 of the inhibition effect for HPA axis then secreted more and more glucocorticoid which resulted in a vicious cycle

515 which could be manifested from atrophy of dendrites and neurons to impaired function of emotion and memory.

516

517

518 **5.   Conclusion**

519   In the present work, metabolic changes in plasma, hippocampus and PFC of CUMS rats was investigated by a

520 UPLC-Orbitrap-MS based metabolomics method. The significantly changed metabolome induced by CUMS

521 procedure revealed the disturbance in neuroendocrinology, amino acid metabolism, energy metabolism, lipid

522 metabolism and synthesis of neurotransmitter. According to the common potential biomarkers in three kinds of

523 samples, we simplified the significantly altered metabolites into a panel which was consist of L-tryptophan,

524 L-kynurenine, quinolinic acid, L-phenylalanine, gamma-aminobutyric acid and N-Acetylaspartic acid. The

525 correlation analysis between the simplified panel in plasma and that of brain obtained a relative good results which

526 indicated that the plasma panel was able to reflect the metabolic changes in brain. According to the metabolic

527 pattern acquired by PCA model, we speculated there was a temporal relation for metabolic changes. Specially,

528 when the simulation of CUMS acted on model rats, it could lead to a series of effects on neuroendocrine and

529 metabolic system which caused the metabolome change in peripheral blood firstly for that blood was circulating

530 through the body constantly. Then the changed level of several metabolites was able to further affect hippocampus,

531 inducing functional or organic changes which might result in a vicious cycle. Finally the metabolic disturbance and

532 the dysfunction of hippocampus probably brought about the damage for PFC. Significantly changed metabolites

533 could support this view and we also gave proper biological interpretation for them in order to match it.

534 Additionally, the predictive power between the metabolome and SP achieved satisfactory results which meant it

535 was practicable to reflect the depressive degree by a metabolomics method. Compared with behavioral test, the

536 changed metabolome was more objective and it could minimize the effect of subjective action for animals during

537 the behavioral test. Even if the test of the simplified panel was not as convenient as behavioral, it was promising to

538 replace behavioral tests gradually for its objectivity with the development of detecting technology. We explored the

539 metabolic changes in three kinds of different samples, and furthermore, it was the first attempt to rank the

540 depressive level in CUMS model by a metabolomics approach in order to explore the relationship between

541 metabolome and severity of depression. These results indicate that it is promising to search for biomarkers for

542 diagnosis by metabolomics method through a noninvasive blood sample rather than cerebrospinal fluid or even

543 biopsy of brain tissue. Additionally, this untargeted metabolomics research would deepen the understanding for

544 MDD in animal models and lay foundation to further studies such as targeted metabolomics research or studies

545 based on human beings.

546

547 **Acknowledgements**

550

551

552

553

554

555

556

557

558

559

560

561

562

563

564

565

566

567

568

569

570

571

572

573 **References**

574 1. N. Bhattarai, J. Charlton, C. Rudisill and M. C. Gulliford, *Psychological medicine*, 2013, **43**,
575 1423-1431.

576 2. P. d'Souza and C. Jago, *Drugs of today (Barcelona, Spain: 1998)*, 2014, **50**, 251-267.

577 3. J. Xuan, G. Pan, Y. Qiu, L. Yang, M. Su, Y. Liu, J. Chen, G. Feng, Y. Fang and W. Jia, *Journal of*
578 *proteome research*, 2011, **10**, 5433-5443.

579 4. X. Liu, P. Zheng, X. Zhao, Y. Zhang, C. Hu, J. Li, J. Zhao, J. Zhou, P. Xie and G. Xu, *Journal of*
580 *proteome research*, 2015, **14**, 2322-2330.

581 5. X. Wang, T. Zhao, Y. Qiu, M. Su, T. Jiang, M. Zhou, A. Zhao and W. Jia, *Journal of proteome*
582 *research*, 2009, **8**, 2511-2518.

583 6. S. R. L. Joca, C. M. Padovan and F. S. Guimarães, *Revista Brasileira de Psiquiatria*, 2003, **25**,
584 46-51.

585 7. P. Willner, *Psychopharmacology*, 1997, **134**, 319-329.

586 8. V. Gupta, R. S. Thakur, C. Reddy and B. Jha, *Rsc Advances*, 2013, **3**, 7037-7047.

587 9. X. Yu, J. Luo, L. Chen, C. Zhang, R. Zhang, Q. Hu, S. Qiao and L. Li, *RSC Advances*, 2015, **5**,
588 69800-69812.

589 10. M. F. Egan, M. Kojima, J. H. Callicott, T. E. Goldberg, B. S. Kolachana, A. Bertolino, E. Zaitsev, B.
590 Gold, D. Goldman and M. Dean, *Cell*, 2003, **112**, 257-269.

591 11. S. Campbell, M. Marriott, C. Nahmias and G. M. MacQueen, *American Journal of Psychiatry*,
592 2014.

593 12. D. Liu, M. Zhang and H. Yin, *International Journal of Neuroscience*, 2013, **123**, 155-162.

594 13. M. N. Potenza, H.-C. Leung, H. P. Blumberg, B. S. Peterson, R. K. Fulbright, C. M. Lacadie, P.
595 Skudlarski and J. C. Gore, *American Journal of Psychiatry*, 2014.

596 14. C. S. Carter, W. Perlstein, R. Ganguli, J. Brar, M. Mintun and J. D. Cohen, 2014.

597 15. T. Zaehle, P. Sandmann, J. D. Thorne, L. Jäncke and C. S. Herrmann, *BMC neuroscience*, 2011,
598 **12**, 2.

599 16. B. T. Denny, H. Kober, T. D. Wager and K. N. Ochsner, *Journal of cognitive Neuroscience*, 2012,
600 **24**, 1742-1752.

601 17. J. Zhao, Y.-H. Jung, C.-G. Jang, K.-H. Chun, S. W. Kwon and J. Lee, *Scientific reports*, 2015, **5**.

602 18. P. Willner, R. Muscat and M. Papp, *Neuroscience & Biobehavioral Reviews*, 1992, **16**, 525-534.

603 19. P. Willner, A. Towell, D. Sampson, S. Sophokleous and R. Muscat, *Psychopharmacology*, 1987,
604 **93**, 358-364.

605 20. E. Choleris, A. Thomas, M. Kavaliers and F. Prato, *Neuroscience & Biobehavioral Reviews*, 2001,
606 **25**, 235-260.

607 21. I. Lucki, *Behavioural pharmacology*, 1997, **8**, 523-532.

608 22. J. Grønli, R. Murison, E. Fiske, B. Bjorvatn, E. Sørensen, C. M. Portas and R. Ursin, *Physiology*
609 *& behavior*, 2005, **84**, 571-577.

610 23. R. N. Walsh and R. A. Cummins, *Psychological bulletin*, 1976, **83**, 482.

611 24. E. Szymańska, E. Saccenti, A. K. Smilde and J. A. Westerhuis, *Metabolomics*, 2012, **8**, 3-16.

612 25. B. Worley, S. Halouska and R. Powers, *Analytical biochemistry*, 2013, **433**, 102-104.

613 26. W. B. Dunn, A. Erban, R. J. Weber, D. J. Creek, M. Brown, R. Breitling, T. Hankemeier, R.
614 Goodacre, S. Neumann and J. Kopka, *Metabolomics*, 2013, **9**, 44-66.

615 27. M. W. Taylor and G. Feng, *The FASEB Journal*, 1991, **5**, 2516-2522.

616 28. J. Savitz, W. C. Drevets, B. E. Wurfel, B. N. Ford, P. S. Bellgowan, T. A. Victor, J. Bodurka, T. K.

617   Teague and R. Dantzer, *Brain, behavior, and immunity*, 2015, **46**, 55-59.

618   29.   M. Heyes, K. Saito, J. Crowley, L. Davis, M. Demitrack, M. Der, L. Dilling, J. Elia, M. Kruesi and A.
619   Lackner, *Brain*, 1992, **115**, 1249-1273.

620   30.   H.-B. Chen, F. Li, S. Wu and S.-C. An, *Sheng li xue bao:[Acta physiologica Sinica]*, 2013, **65**,
621   577-585.

622   31.   L. R. Orlando, S. A. Alsdorf, J. B. Penney and A. B. Young, *Experimental neurology*, 2001, **167**,
623   196-204.

624   32.   D. Zádori, G. Nyiri, A. Szőnyi, I. Szatmári, F. Fülöp, J. Toldi, T. F. Freund, L. Vécsei and P. Klivényi,
625   *Journal of neural transmission*, 2011, **118**, 865-875.

626   33.   Z. Hartai, A. Juhász, Á. Rimanóczy, T. Janáky, T. Donkó, L. Dux, B. Penke, G. K. Tóth, Z. Janka
627   and J. Kálmán, *Neurochemistry international*, 2007, **50**, 308-313.

628   34.   A. Clacy, R. Sharman and J. McGill, *Journal of Developmental & Behavioral Pediatrics*, 2014,
629   **35**, 388-391.

630   35.   I. H. Miklós and K. J. Kovács, *Biological psychiatry*, 2012, **71**, 301-308.

631   36.   E. Küçükibrahimoğlu, M. Z. Saygın, M. Çalışkan, O. K. Kaplan, C. Ünsal and M. Z. Gören,
632   *European journal of clinical pharmacology*, 2009, **65**, 571-577.

633   37.   C. Gasparovic, N. Arfai, N. Smid and D. M. Feeney, *Journal of neurotrauma*, 2001, **18**, 241-246.

634   38.   R. J. Steingard, D. A. Yurgelun-Todd, J. Hennen, J. C. Moore, C. M. Moore, K. Vakili, A. D. Young,
635   A. Katic, W. R. Beardslee and P. F. Renshaw, *Biological psychiatry*, 2000, **48**, 1053-1061.

636   39.   C. Tsigos and G. P. Chrousos, *Journal of psychosomatic research*, 2002, **53**, 865-871.

637   40.   G. Chrousos, *International journal of obesity and related metabolic disorders: journal of the*
638   *International Association for the Study of Obesity*, 2000, **24**, S50-55.

639   41.   C. L. Burton, D. Chatterjee, M. Chatterjee-Chakraborty, V. Lovic, S. L. Grella, M. Steiner and A.
640   S. Fleming, *Brain research*, 2007, **1158**, 28-38.

641

642

643

644

645

646

647

648

649

650

651

652

653

654

655

Figure Legends

657   **Fig.1** Experimental design for the present study.

658

659   **Fig.2** The results of behavioral tests for SPT (a), OPT (b,c) and FST (d) of the control, model, and treated group.

660   Data are represented as mean±SD.

661   * means a statistically significant difference at p<0.05, ** means a statistically significant difference p<0.01

662

663

664   **Fig.3** The PCA and PLS-DA score plot in plasma (a), hippocampus (b) and PFC (c). The left side is the PCA score

665   plot and the right side is the PLS-DA score plot conducted by the dataset of three groups.

666

667   **Fig.4** The scatter diagrams of each metabolites in the simplified panel in plasma.

668

669   **Fig.5** The diagram of linear-regression analysis between SP and the level of metabolites in the simplified panel in

670   plasma.

671

672   **Fig.6** The plots of newly-conducted predictive PLS-DA model of plasma. The left side is the score plot conducted

673   by the training set (control and model group) $R2X\ (cum)=0.686$, $R^2Y\ (cum)=0.994$, $Q^2\ (cum)=0.748$; in the middle is the

674   predicted plot from PLS-DA model, the X axis is the predicted SP and the Y axis is the real SP; on the right side is

675   the 50-iteration permutation test, showing that the values of permuted R^2 and Q^2 (bottom left) are significantly

676   lower than the corresponding original R^2 and Q^2 values (top right).

677

678   **Fig.7** The perturbed metabolic pathways in response to CUMS procedure and treatment of paroxetine.

679
680
681
682
683
684
685
686

687

688

689   **Table.1** The parameters for assessing the modeling quality of PLS-DA model in plasma, hippocampus and PFC samples

690

	Components	PLS-DA		
		$R^2X\ (cum)^a$	$R^2Y\ (cum)^a$	$Q^2\ (cum)^b$
Plasma samples	4	0.441	0.994	0.748
Hippocampus samples	4	0.397	0.993	0.686
PFC samples	4	0.353	0.991	0.653

691   a.R^2X (cum) and bR^2Y (cum) represent the cumulative Sum of Squares (SS) of all the X's and Y's explained by all extracted components

692   b.Q^2Y (cum) is an estimate of how well the model predicts the Y's.

693

694

Table.2 Potential biomarkers characterized in the plasma profile and their change trends in different groups (n = 10 in each group)

No	Metabolite	m/z(amu)	t_R(min)	VIP[c] score	Model vs. Control		Model vs. Treat		Corresponding metabolic pathway
					fold change[d]	p-value	fold change[d]	p-value	
1	L-Phenylalanine[a]	165.0785	2.53	1.87	1.55	9.31E-09	1.14	0.019	Synthesis of neurotransmitter
2	Gamma-Aminobutyric acid[a]	103.0631	7.04	2.19	0.49	2.04E-09	0.71	3.22E-04	Synthesis of neurotransmitter
3	L-Tryptophan[a]	204.0901	4.54	1.83	0.54	3.45E-08	0.68	1.90E-04	Tryptophan metabolism
4	Glycine[a]	75.03179	0.91	1.78	0.52	5.23E-08	0.74	0.013	Glycine and serine metabolism
5	Dopamine[a]	153.0785	1.08	1.73	0.50	1.25E-06	0.67	N.S.	Synthesis of neurotransmitter
6	Beta-Alanine[a]	89.04808	6.92	1.77	0.72	1.91E-06	0.83	0.02	Alanine metabolism
7	Azelaic acid[a]	188.1058	1.51	1.77	0.68	2.95E-06	0.87	4.17E-03	Antioxidant
8	Myoinositol[a]	180.0626	0.67	1.69	0.38	3.56E-06	0.81	N.S.	Galactose metabolism
9	Glucose[a]	180.0631	0.65	1.51	0.43	9.63E-06	0.87	N.S.	Energy metabolism
10	L-Kynurenine[a]	208.0844	5.85	1.79	2.27	2.04E-05	1.55	3.84E-03	Tryptophan metabolism
11	Hypoxanthine[a]	136.0392	0.65	1.43	0.47	5.21E-05	0.70	N.S.	Purine metabolism
12	Glycerol[a]	92.04758	0.94	1.70	0.65	9.45E-05	0.87	N.S.	Glycerolipid metabolism
13	Quinolinic acid[a]	167.0213	0.94	1.51	1.75	1.81E-04	1.35	6.15E-03	Tryptophan metabolism
14	Kynurenic acid[a]	187.0276	0.69	1.42	0.53	1.91E-04	0.78	8.25E-03	Tryptophan metabolism
15	N-Acetyl-L-aspartic acid[a]	175.0480	4.28	1.64	1.88	2.12E-04	1.26	5.23 E-03	Synthesis of neurotransmitter
16	Citric acid[a]	192.0261	1.08	1.39	0.76	4.53E-04	0.87	0.015	Energy metabolism
17	PC(14:0)[b]	757.5612	11.10	1.48	1.96	5.31E-04	1.53	0.024	Lipid metabolism
18	LysoPE(20:0)[b]	509.3476	9.59	1.60	1.56	5.51E-04	1.25	5.95 E-03	Lipid metabolism
19	PC(16:0)[b]	807.5751	10.63	1.33	0.60	8.71E-04	1.08	N.S.	Lipid metabolism
20	Sorbitol[a]	182.0788	5.33	1.45	0.67	9.58E-04	0.82	0.011	Galactose metabolism
21	LysoPC(20:5)[b]	541.3153	8.56	1.77	1.46	1.63E-03	0.93	N.S.	Lipid metabolism
22	Corticosterone[a]	346.2146	6.85	1.59	1.36	4.52E-04	1.13	N.S.	Hormone metabolism
23	LysoPC(22:6)[b]	567.3326	8.86	1.51	1.73	3.89E-03	1.40	0.011	Lipid metabolism

24	LysoPC(20:4)[b]	543.3318	8.92	1.37	1.29	6.42E-03	1.13	N.S.	Lipid metabolism
25	LysoPE(16:0)[b]	453.2844	9.15	1.28	1.35	7.16E-03	1.20	0.010	Lipid metabolism

695

696   a Metabolites identified by comparing with authentic standards available in our in-house library.

697   b Metabolites identified by comparing with the HMDB database.

698   c.Variable importance in the projection (VIP) values were obtained from cross-validated PLS-DA models with a threshold of 1.

699   d. Fold change was calculated as the ratio of the mean metabolite levels between two groups.

700

701

702

703

704

705

706

707

708

709

710

711

712 **Table.3** Potential biomarkers characterized in the hippocampus profile and their change trends in different groups (n = 10 in each group)

No	Metabolite	m/z(amu)	t_R(min)	VIP[c] score	Model vs. Control		Model vs. Treat		Corresponding metabolic
					fold change[d]	p-value	fold change[d]	p-value	pathway
1	L-Tryptophan[a]	204.0902	4.46	1.97	0.54	3.13E-07	0.76	7.85E-04	Tryptophan metabolism
2	L-Tyrosine[a]	181.0736	1.04	1.93	0.70	6.40E-07	0.83	6.77E-03	Tyrosine biosynthesis
3	Citric acid[a]	192.0266	1.02	1.73	0.69	1.57E-06	0.89	N.S.	Energy metabolism
4	L-Valine[a]	117.0791	5.22	1.63	0.57	4.07E-06	0.79	0.038	Valine and isoleucine biosynthesis
5	N-Acetyl-L-aspartic acid[a]	175.0482	4.43	1.85	0.55	4.37E-06	0.79	6.63E-03	Synthesis of neurotransmitter
6	Dihydroxyacetone phosphate[b]	169.9974	0.86	1.61	0.63	6.62E-06	0.82	6.79E-03	Glycerolipid metabolism
7	L-Kynurenine[a]	208.0838	5.96	1.76	1.29	8.77E-06	1.17	5.91E-03	Tryptophan metabolism
8	Quinolinic acid[a]	167.0220	0.90	1.47	1.62	5.19E-05	1.29	0.019	Tryptophan metabolism
9	Inosine[a]	268.0806	1.87	1.72	1.40	7.08E-05	1.20	3.59E-03	Inositol phosphate metabolism
10	Glutathione[a]	307.0838	0.98	1.66	1.34	8.89E-05	1.14	3.81E-03	Cysteine metabolism
11	LysoPE(18:0)[b]	481.3168	9.80	1.51	1.48	9.94E-05	1.08	0.410	Lipid metabolism
12	LysoPC(16:0)[b]	495.3325	9.20	1.48	1.33	1.52E-04	1.15	0.031	Lipid metabolism
13	3-Hydroxy-hexadecanoic acid[a]	272.2360	5.07	1.65	0.53	3.40E-04	0.74	7.37E-03	Lipid metabolism
14	L-Isoleucine[a]	131.0949	1.23	1.44	0.51	3.90E-04	0.66	9.77E-03	Valine and isoleucine biosynthesis
15	L-Phenylalanine[a]	165.0785	2.50	1.68	1.65	5.68E-04	1.40	2.45E-03	Synthesis of neurotransmitter
16	Myoinositol[a]	180.0623	0.62	1.46	1.26	7.41E-04	1.06	0.045	Inositol phosphate metabolism
17	Gamma-Aminobutyric acid[a]	103.0635	6.90	1.58	0.81	9.32E-04	0.92	N.S.	Synthesis of neurotransmitter
18	Glycerol[a]	92.0474	0.92	1.27	0.70	9.42E-04	0.87	N.S.	Glycerolipid metabolism
19	L-Serine[a]	105.0427	1.72	1.53	0.63	1.43E-03	0.78	0.013	Glycine and serine metabolism
20	LysoPE(16:0)[b]	453.2854	9.10	1.40	1.34	2.22E-03	1.08	N.S.	Lipid metabolism
21	Homocysteine[a]	135.0357	1.98	1.58	1.19	5.43E-03	1.07	N.S.	Cysteine metabolism
22	Succinic acid[a]	118.0273	1.42	1.35	0.55	5.69E-03	0.79	0.024	Energy metabolism
23	Beta-Alanine[a]	89.0481	7.01	1.28	1.31	7.03E-03	1.07	N.S.	Alanine metabolism

713   a Metabolites identified by comparing with authentic standards available in our in-house library.

714   b Metabolites identified by comparing with the HMDB database.

715   c.Variable importance in the projection (VIP) values were obtained from cross-validated PLS-DA models with a threshold of 1.

716   d. Fold change was calculated as the ratio of the mean metabolite levels between two groups.

717

718

719

720

721

722

723

724

725

726

727

728

729

730

731

732 **Table.4** Potential biomarkers characterized in the PFC profile and their change trends in different groups (n = 10 in each group)

No	Metabolite	m/z(amu)	t_R(min)	VIP[c] score	Model vs. Control fold change[d]	p-value	Model vs. Treat fold change[d]	p-value	Corresponding metabolic pathway
1	Kynurenic acid[a]	189.0428	0.73	1.93	0.53	1.14E-06	0.70	7.21E-04	Tryptophan metabolism
2	L-Tryptophan[a]	204.0897	4.46	1.88	0.73	1.45E-05	0.82	3.77E-03	Tryptophan metabolism
3	Dopamine[a]	153.0787	0.96	1.82	0.67	1.24E-04	0.80	8.33E-03	Synthesis of neurotransmitter
4	Quinolinic acid[a]	167.0210	0.99	1.84	1.56	1.35E-04	1.25	2.51E-03	Tryptophan metabolism
6	Inosine[a]	268.0806	1.90	1.80	1.66	1.48E-04	1.12	N.S.	Inositol phosphate metabolism
7	Linolenic acid[a]	278.2240	8.99	1.54	1.16	1.56E-04	1.07	N.S.	Alpha-Linolenic acid metabolism
8	L-Dopa[a]	197.0683	0.75	1.78	0.72	5.01E-04	0.87	0.021	Synthesis of neurotransmitter
9	5-Hydroxyindoleacetic acid[a]	191.0588	0.81	1.71	0.59	5.42E-04	0.72	2.36E-03	Tryptophan metabolism
10	N-Acetyl-L-aspartic acid[a]	175.0478	4.45	1.80	0.66	8.41E-04	0.78	0.031	Synthesis of neurotransmitter
11	Docosahexaenoic acid[a]	328.23906	5.78	1.52	0.80	1.27E-03	0.92	0.039	Lipid metabolism
12	L-Isoleucine[a]	131.0948	1.24	1.57	0.61	1.34E-03	0.76	8.79E-03	Leucine and isoleucine biosynthesis
13	Gamma-Aminobutyric acid[a]	103.0638	7.09	1.48	0.71	1.89E-03	0.86	N.S.	Synthesis of neurotransmitter
14	Homovanillic acid[a]	182.0583	0.68	1.61	0.68	2.64E-03	0.85	N.S.	Tyrosine metabolism
15	L-Kynurenine[a]	208.0846	5.98	1.55	1.39	3.54E-03	1.18	0.033	Tryptophan metabolism
16	L-Phenylalanine[a]	165.0789	2.52	1.57	1.41	5.40E-03	1.15	0.015	Synthesis of neurotransmitter
17	L-Lysine[a]	146.1069	5.27	1.74	2.39	6.38E-03	1.72	0.010	Biotin Metabolism
18	Tyramine[a]	137.0840	9.65	1.37	1.28	8.37E-03	1.18	0.048	Tyrosine metabolism
19	L-Tyrosine[a]	181.0738	1.05	1.32	0.60	0.011	0.71	N.S.	Tyrosine metabolism
20	L-Aspartic acid[a]	133.0366	1.14	1.25	1.53	0.016	1.07	N.S.	Alanine metabolism

733   a Metabolites identified by comparing with authentic standards available in our in-house library.

734   b Metabolites identified by comparing with the HMDB database.

735   c.Variable importance in the projection (VIP) values were obtained from cross-validated PLS-DA models with a threshold of 1.

736   d. Fold change was calculated as the ratio of the mean metabolite levels between two groups.

737   **Table.5** Pearson's coefficient values of metabolites in different samples

738

739

	Plasma v.s. Hippocampus		Plasma v.s. PFC	
Metabolite	r	p-value	r	p-value
L-Tryptophan	0.8143	p<0.001	0.7089	p<0.001
L-Kynurenine	0.6491	P=0.002	0.6145	p=0.003
Quinolinic acid	0.6674	P=0.001	0.6122	P=0.003
L-Phenylalanine	0.8102	p<0.001	0.5788	P=0.006
Gamma-Aminobutyric acid	0.8593	p<0.001	0.7157	p<0.001
N-Acetyl-L-aspartic acid	-0.6613	p=0.006	-0.5983	P=0.002

748

749

750

751

752   **Table.6** Pearson's coefficient values and p-values obtained from the binary logistic regression

	Plasma vs. Sucrose Preference	
Metabolite	r	p-value
L-Tryptophan	0.8187	p<0.001
L-Kynurenine	-0.6969	p=0.002
Quinolinic acid	-0.7298	p=0.002
L-Phenylalanine	-0.7898	p<0.001
Gamma-Aminobutyric acid	0.7910	p<0.001
N-Acetyl-L-aspartic acid	-0.7421	p=0.001

753

754

755

756

757

758
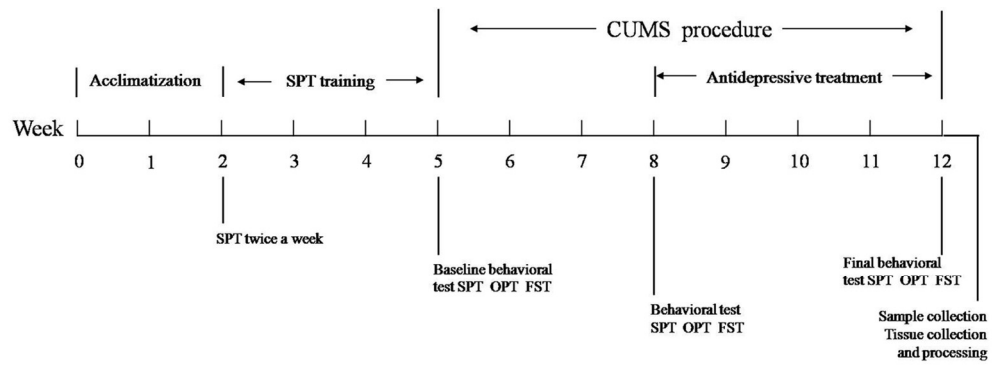
63x22mm (600 x 600 DPI)
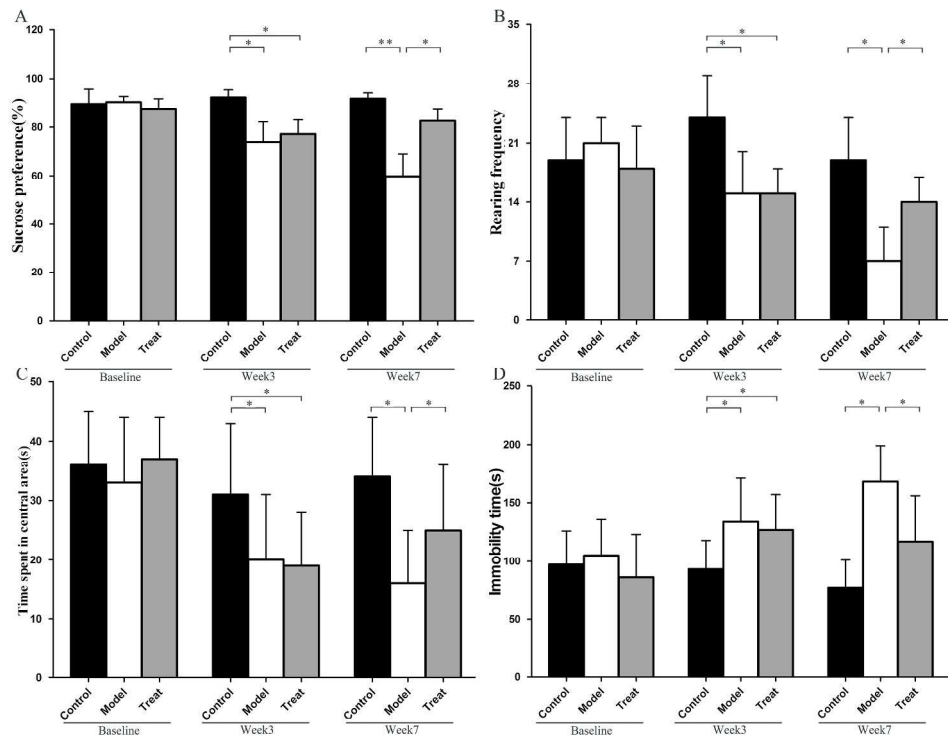
133x100mm (600 x 600 DPI)
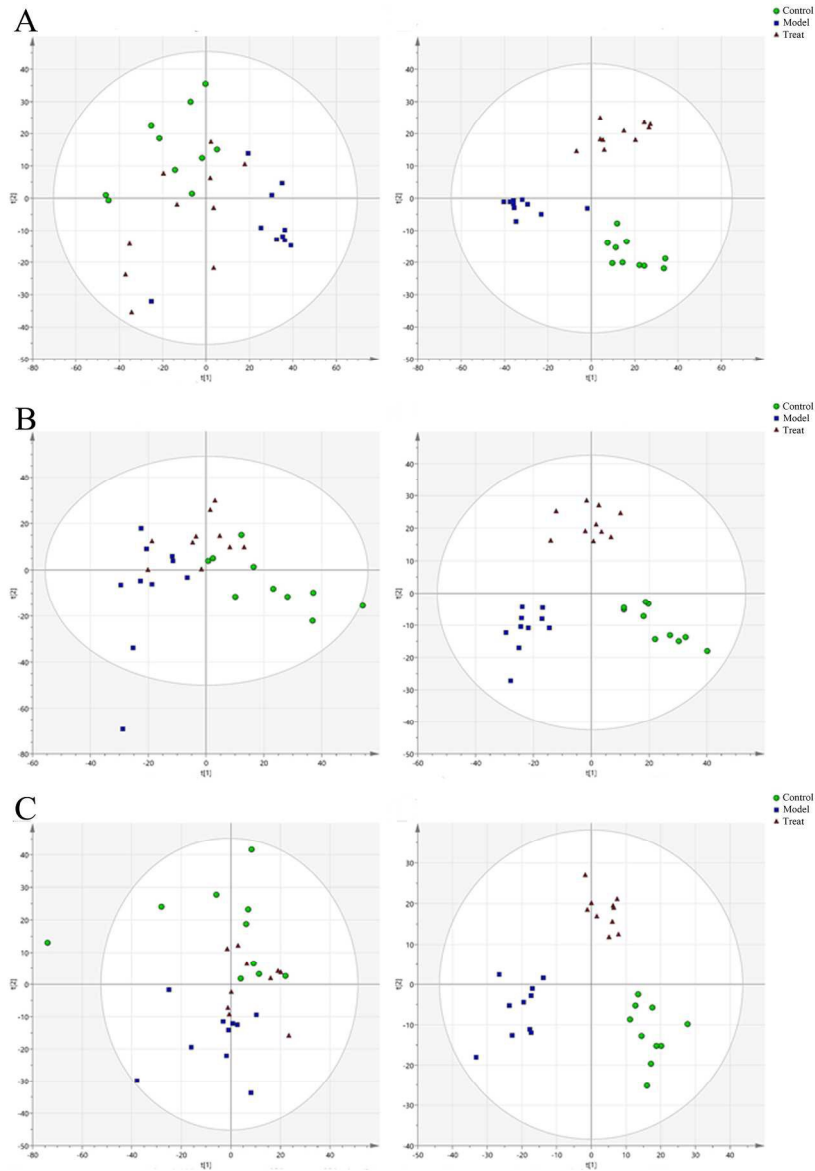
119x173mm (600 x 600 DPI)
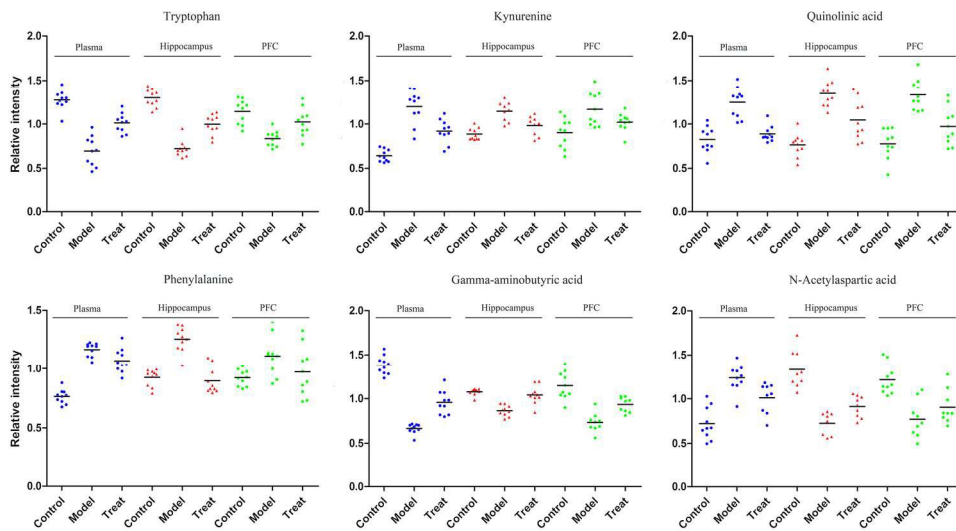
97x53mm (600 x 600 DPI)
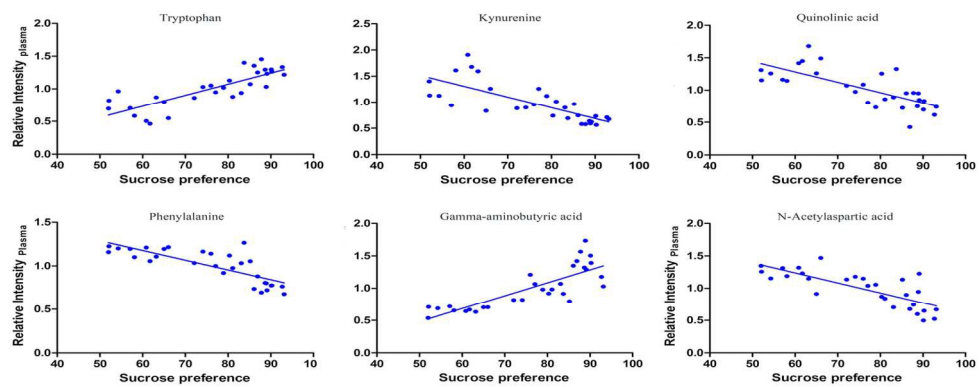
69x27mm (600 x 600 DPI)
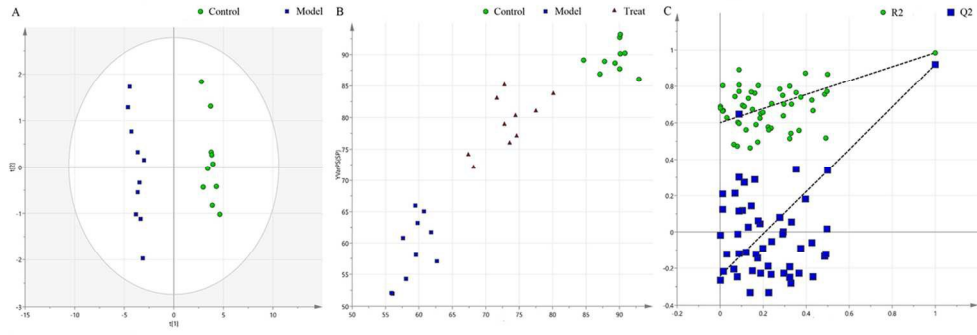
60x20mm (600 x 600 DPI)
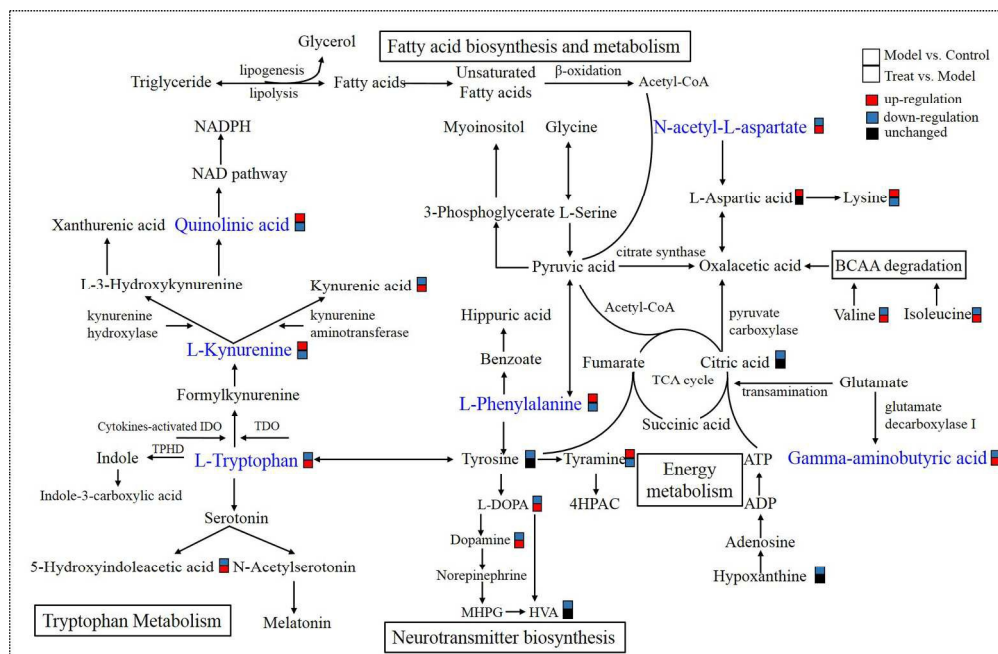
114x73mm (600 x 600 DPI)

Graphic abstract